Hindawi
Journal of Food Quality
Volume 2024, Article ID 6802701, 14 pages
https://doi.org/10.1155/2024/6802701

Research Article

Modified Gegen Qinlian Decoction Ameliorates DSS-Induced Ulcerative Colitis in Mice by Inhibiting Ferroptosis via Nrf2/GPX4 Pathway

Jinke Huang, Jiaqi Zhang, Zhihong Liu, Jing Ma, Fengyun Wang, and Xudong Tang

Institute of Digestive Diseases, Xiyuan Hospital of China Academy of Chinese Medical Sciences, Beijing, China

Correspondence should be addressed to Xudong Tang; txdly@sina.com

Received 13 November 2023; Revised 16 January 2024; Accepted 22 January 2024; Published 7 February 2024

Academic Editor: Muhammad Babar Khawar

Copyright © 2024 Jinke Huang et al. This is an open access article distributed under the Creative Commons Attribution License, which permits unrestricted use, distribution, and reproduction in any medium, provided the original work is properly cited.

Objective. Ferroptosis, a form of programmed cell death, is considered a novel target for the treatment of ulcerative colitis (UC). The aim of this study was to explore whether modified Gegen Qinlian decoction (MGQD) ameliorates UC in mice via mediating ferroptosis. *Methods*. Mice with dextran sulfate sodium- (DSS-) induced colitis were administered with MGQD for seven days. Subsequently, iron, malondialdehyde (MDA), glutathione (GSH), and reactive oxygen species (ROS) were measured. ELISA and immunohistochemistry were used to evaluate the levels of proinflammatory cytokines and tight junction proteins, respectively. Transmission electron microscopy was used to reveal mitochondrial morphology. Western blot and qRT-PCR analyses were used to assess the expression levels of the proteins of Nrf2/GPX4 pathway. The docking affinity of MGQD and Nrf2 was assessed using AutoDock Vina 1.1.2. *Results*. Ferroptosis was identified in mice with UC, as demonstrated by mitochondrial disruption, MDA and ROS production, iron overload, decrease in GSH level, and abnormal expression of core marker proteins of ferroptosis. After MGQD treatment, these characteristic changes of ferroptosis were significantly reversed, along with concomitant activation of the Nrf2/GPX4 pathway. Furthermore, molecular docking analysis revealed that MGQD had a high affinity for Nrf2. *Conclusion*. MGQD may ameliorate UC by inhibiting ferroptosis via the activation of Nrf2/GPX4 pathway. This study provided new insights into the application of MGQD complementary therapy for UC.

1. Introduction

Ulcerative colitis (UC) is a common inflammatory bowel disease [1]. The incidence of UC has been increasing continuously worldwide, imposing a significant economic burden on society [2]. The etiology of UC remains poorly understood, although environmental factors, genetics, immune responses, and intestinal microflora have been implicated as causative factors for UC [1]. Currently, the therapies for UC are focused on controlling the active inflammatory response and regulating intestinal immune balance, and commonly used drugs include 5-aminosalicylic acid drugs, immunosuppressants, and steroids [3, 4]. However, the long-term use of these drugs poses the challenges of significant adverse events and drug resistance [5, 6]. Therefore, it is urgent to develop potent medications for UC.

Ferroptosis is a newly discovered type of programmed cell death caused by oxidative stress and high reactive oxygen species (ROS) production [7]. The death of epithelial cells in UC has recently been linked to ferroptosis, and inhibition of ferroptosis has been demonstrated to be beneficial for UC [8, 9]. Nrf2 is a transcription factor involved in the resistance to endogenous oxidative stress. Genes located downstream of Nrf2 play roles in key regulatory functions in iron metabolism (FTH1, FTL, SLC40A1, MT1G, and FECH), ROS accumulation (GPX4, HO-1, and NQO1), and GSH production (GSR, GCLC, GSS, and SLC7A11). Thus, activation of Nrf2/GPX4 pathway is a classical strategy to inhibit ferroptosis [10, 11].

Gegen Qinlian decoction (GQD) is a well-known Chinese herbal formula beneficial for UC [12]. Our previous study reported that modified GQD (MGQD) is efficacious in alleviating UC in mice [13–15]. Intestinal epithelial cell death can promote the pathological progression of UC by altering the integrity of the intestinal barrier [16]. Therefore, in this study, we aimed to further investigate the mechanism underlying the therapeutic action of MGQD in UC via ferroptosis regulation.

2. Materials and Methods

2.1. Decoction Preparation. The composition of MGQD is as follows: *Coptidis Rhizoma* (9 g), *Radix Puerariae* (24 g), *Zingiberis Rhizoma* (9 g), *Scutellariae Radix* (9 g), *Talcum* (9 g), and *Liquorice* (6 g). MGQD was provided by the pharmacy of Xiyuan Hospital of China Academy of Chinese Medical Sciences. MGQD extracts were prepared as per the standard for preparing the decoction of Chinese herbal medicines. The production process was as follows. The herbs were soaked in distilled water (1 : 8, w/v) for 1 h. *Talcum* was boiled in distilled water for 30 min before adding the rest of the herbs for 1.5 h and then filtered. The residue was combined with six times the amount of distilled water and boiled for 1 h, followed by filtration. The two filtrates were mixed, and crude drug of concentrations 0.5, 1, and 2 g/mL was prepared.

2.2. Animal Experimental Protocol. C57BL/6J mice (weighing 18–22 g) provided by SPF Biotech (Beijing, China) were randomly allocated into six groups: control, dextran sulfate sodium (DSS), medium-dose MGQD (GM), low-dose MGQD (GL), high-dose MGQD (GH), and ferroprostatin-1 (Fer-1; a ferroptosis inhibitor) ($n = 10$/group). Except the control group, other five groups received 3% (w/v) DSS diluted in drinking water for 7 days to induce acute experimental UC. At the same time, the GL, GM, and GH groups orally received 5, 10, and 20 mg/kg MGQD once per day for 7 consecutive days. The MGQD dose used here was calculated based on the clinical dose of raw materials. For the Fer-1 group, every other day from the day before DSS induction, the ferroptosis inhibitor Fer-1 (HY-100579, MedChemExpress, USA) was administered intraperitoneally to mice. The control and DSS groups intragastrically received the same dosages of distilled water. On day 8, all mice were sacrificed under anesthesia using ether, and the length of the colon was measured. The detailed experimental procedure is presented in Figure 1(a).

2.3. Histological Analysis. For hematoxylin and eosin (H&E) staining, colon samples were embedded in paraffin, fixed in 4% paraformaldehyde, and cut into 5 m thick blocks. Based on previously established standards, a blinded assessment of the colitis activity was performed using the sections stained with H&E [13–15].

2.4. Transmission Electron Microscopy. Fresh colorectal tissue samples of mice were fixed in glutaraldehyde. The samples were dehydrated using various concentrations of ethanol, followed by washing multiple times with phosphate buffer saline. The samples were dehydrated, thinly sliced, and inserted into the resin. The sections were stained with 0.5% lead citrate and 4% uranyl acetate, and images were captured using transmission electron microscopy.

2.5. Measurement of the Levels of Proinflammatory Cytokines. The levels of IFN-γ, IL-6, IL-1β, and TNF-α in colonic tissues of mice with UC were determined using respective ELISA kits as per the manufacturer's instructions (Ruixin Biotechnology Co., Ltd., Quanzhou, China).

2.6. Immunohistochemistry. Tight junction protein concentration in colonic tissues of mice with UC was measured using immunohistochemistry. The slices were incubated with ZO-1 (1 : 100; Affinity Biosciences; AF5145), occludin (1 : 200; Proteintech; 28674-1-AP), claudin-1 (1 : 200; Proteintech; 28674-1-AP), and 4HNE (1 : 1000; Bio-Techne; MAB3249) antibodies overnight at 4°C, followed by incubation with the secondary antibody (1 : 200; Servicebio; GB23303). The images of stained samples were taken using a light microscope (Olympus BX41, Shanghai, China). The mean optical density value was used to analyze and represent staining intensity.

2.7. Western Blot Analysis. Proteins from the colon tissue samples were extracted and separated as per their molecular weights using 10% SDS-PAGE. The membrane was incubated with the primary antibodies for Nrf2 (1 : 3000, Proteintech, 16396-1-ap), GPX4 (1 : 3000, Proteintech, GB113091), FTH1 (1 : 3000, Proteintech, GB112933), ACSL4 (1 : 3000, Servicebio, GB113871), SLC7A11 (1 : 3000, Proteintech, 26864-1-ap), and GAPDH (1 : 5000, Servicebio, GB15002) overnight at 4°C. Furthermore, the membrane was incubated with HRP-labeled rabbit or mouse IgG secondary antibodies (1 : 5000, Servicebio, GB23303 and GB25301) for 2 h at room temperature. The protein signals were visualized using ECL solution (P0018, Beyotime).

2.8. Measurement of Iron Content and Levels of GSH, MDA, and ROS. After extraction of protein samples from the colonic tissues, the levels of malondialdehyde (MDA), glutathione (GSH), reactive oxygen species (ROS), and iron were measured using respective kits as per the manufacturer's instructions (Ruixin Biotechnology Co., Ltd., Quanzhou, China).

2.9. RT-qPCR Analysis. Total RNA was extracted from the colon tissue and used to synthesize cDNA using reverse transcription. RT-qPCR was performed using the CFX96 real-time PCR detection system (Bio-Rad, USA). GAPDH was used as the internal control. The relative expression levels of target genes were determined using $2^{-\Delta\Delta CT}$ method. The primer sequences are given in Table 1.

2.10. Macromolecular Docking. Baicalin, puerarin, palmatine chloride, wogonin, and berberine chloride were identified as the main components of MGQD in our previous

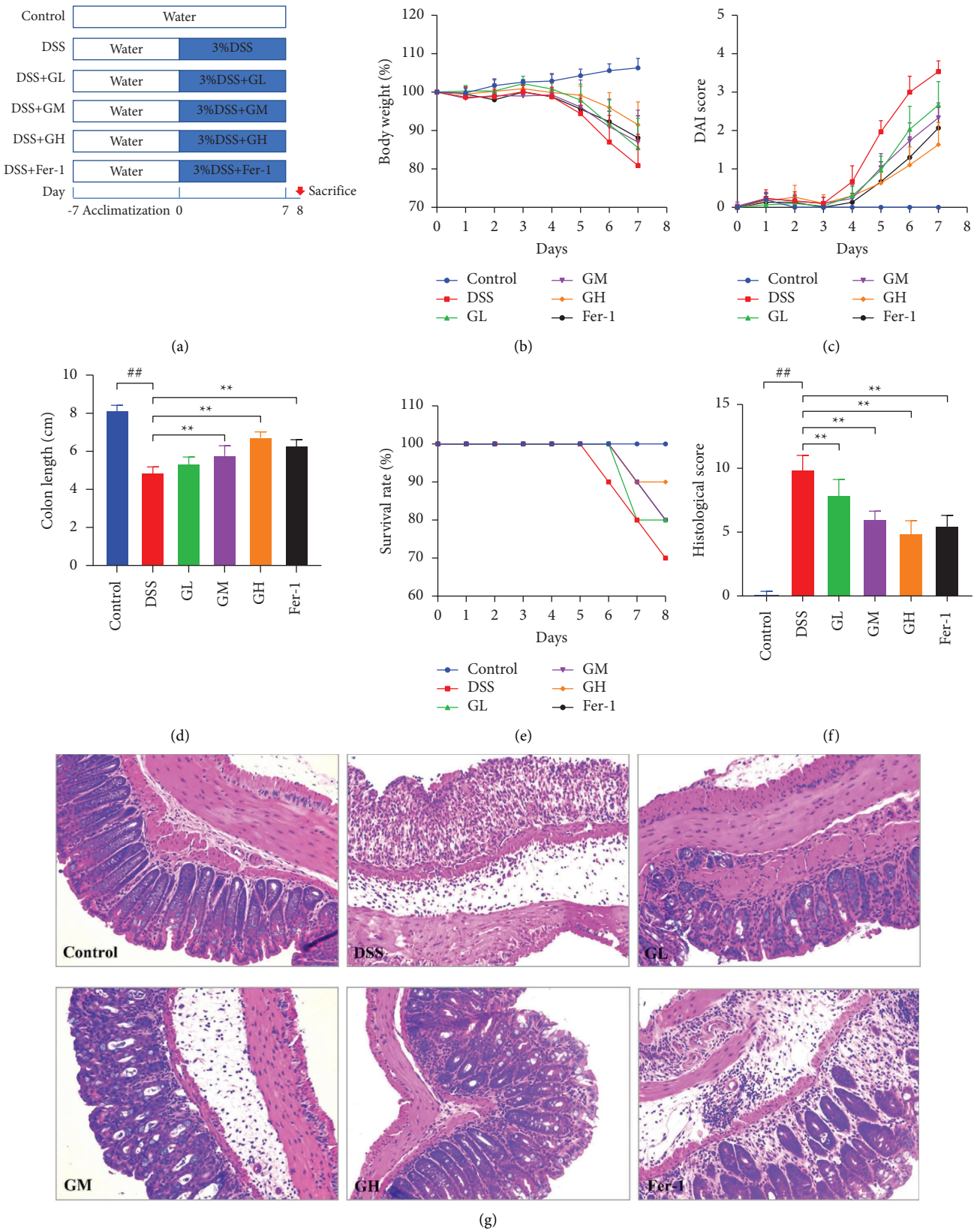

FIGURE 1: MGQD ameliorated colitis induced by DSS in mice. (a) The experimental protocol, (b) daily changes in body weight in different groups, (c) daily changes in DAI score in different groups, (d) comparison of colon length, (e) survival rate of mice in each group, and (f, g) representative H&E staining images of colon sections and the comparison of histopathological scores (200x magnification). $^{\#\#}P < 0.005$ vs. control; $^{**}P < 0.005$ vs. DSS.

Table 1: Primer sequences.

Genes	Forward primer	Reverse primer
Nrf2	TGTCTTAATACCGAAAACAAGCAGC	GACCACAGTTGCCCACTTCTTTT
GPX4	GCACATGGTCTGCCTGGATAAG	TCTTGATTACTTCCTGGCTCCTG
GAPDH	CCTCGTCCCGTAGACAAAATG	TGAGGTCAATGAAGGGGTCGT

study via high-performance liquid chromatography system [13]. In this study, the molecular docking of the components of MGQD and Nrf2 was performed using AutoDock Vina 1.1.2. The structure of component was obtained using the PubChem database. Energy minimization of the components and conversion of their 2D structures into 3D chemical structures were performed using ChemBio3D 13.0 software. The crystal structure of the Nrf2 domain was used as the receptor model, and the 3D structure was obtained using PDB database.

2.11. Statistical Analysis. All continuous data were expressed as mean ± standard deviation. Before analysis, normality and variance homogeneity tests were performed for each set of data to be compared. For comparisons of more than two groups, one-way or two-way analysis of variance was performed, with Bonferroni's or Dunnett's multiple-comparisons test for normally distributed data or the Mann–Whitney test for nonnormally distributed data. Unless otherwise stated, $P < 0.05$ was considered significant. Statistical analyses were performed using SPSS 26.0 and GraphPad Prism version 9 software.

3. Results

3.1. MGQD Attenuated UC in Mice. On day 4 of the experiments, weight of the mice with UC was significantly lower (Figure 1(b)) and the disease activity index (DAI) was significantly higher (Figure 1(c)), compared with mice in the control group. Similarly, the length of the colon was significantly shorter in mice with UC (Figure 1(d)). In addition, mice with DSS-induced UC exhibited mortality rate of 30%. After MGQD treatment, the mortality rate of mice with UC was reduced, particularly the survival rate of mice in the GH group significantly improved to 90% (Figure 1(e)).

Pathological results revealed that the mice in the control group had clear crypt structure and intact colonic mucosa, whereas the colonic histopathological damage was obvious in the mice with UC with extensive infiltration of inflammatory cells, crypt structure, and severe disorganization of the mucosa (Figures 1(f) and 1(g)). Surprisingly, all the aforementioned alterations in mice with UC were reversed by MGQD and Fer-1 treatment, and the most significant improvement in clinical symptoms in the mice with UC was observed at a dose of 20 g/kg MGQD (Figures 1(b)–1(g)).

3.2. MGQD Suppressed Proinflammation in Mice with UC. High levels of IFN-γ, IL-1β, IL-6, and TNF-α were observed in the colonic tissues of mice with UC compared with the control mice (Figures 2(a)–2(d)). Surprisingly, the levels of these proinflammatory cytokines were dramatically reduced in colonic tissues after MGQD and Fer-1 treatments (Figures 2(a)–2(d)).

3.3. MGQD Enhanced the Intestinal Barrier Function of Mice with UC. UC is pathologically characterized by inflammation of the intestinal mucosa and disruption of intestinal barrier function [1]. Continued deterioration of ferroptosis will lead to disruption of intestinal barrier function, which is characterized by suppression of the expression of tight junction proteins [8, 16]. Tight junction proteins such as claudin-1, ZO-1, and occludin were therefore detected by immunohistochemistry in this study, and results suggested that the expression of claudin-1, ZO-1, and occludin was suppressed in the colonic tissues of mice with UC compared with the control mice (Figures 3(a)–3(f)). Interestingly, mice treated with MGQD exhibited an increased expression of claudin-1, ZO-1, and occludin in a dose-dependent manner (Figures 3(a)–3(f)). Furthermore, the expressions of these proteins were comparable in the Fer-1 and GH groups (Figures 3(a)–3(f)).

3.4. MGQD Inhibited Ferroptosis in Mice with UC. Transmission electron microscopic results revealed that the colonic tissues of mice with UC exhibited reduced mitochondrial size, membrane density, and cristae and apparent rupture of the outer membranes compared with the control. Interestingly, the mitochondria in the MGQD and Fer-1 groups were relatively normal, and the cristae were clear (Figure 4).

Furthermore, elevated levels of Fe^{2+}, ROS, and MDA and decreased levels of GSH and Fe^{3+} were observed in mice with UC (Figures 5(a)–5(e)). Interestingly, these abnormal results were considerably reversed by MGQD and Fer-1 treatments (Figures 5(a)–5(e)). In addition, 4HNE expression was higher in colonic tissues of mice with UC but was inhibited by MGQD and Fer-1 treatments (Figure 6).

Western blot analysis (Figure 7) revealed that SCL7A11 and FTH1 were downregulated, whereas ACSL4 was upregulated in the colonic tissues of mice with UC compared with the control group. However, after MGQD treatment, all these changes were reversed. Notably, ferroptosis was inhibited to the highest level when the dose of MGQD was 20 mg/kg.

3.5. MGQD Activated the Nrf2/GPX4 Pathway in the Colonic Tissues of Mice with UC. Western blot and RT-qPCR analyses revealed that protein and mRNA levels of Nrf2 and GPX4 were significantly reduced in the colonic tissues of mice with UC compared with the control group (Figure 8).

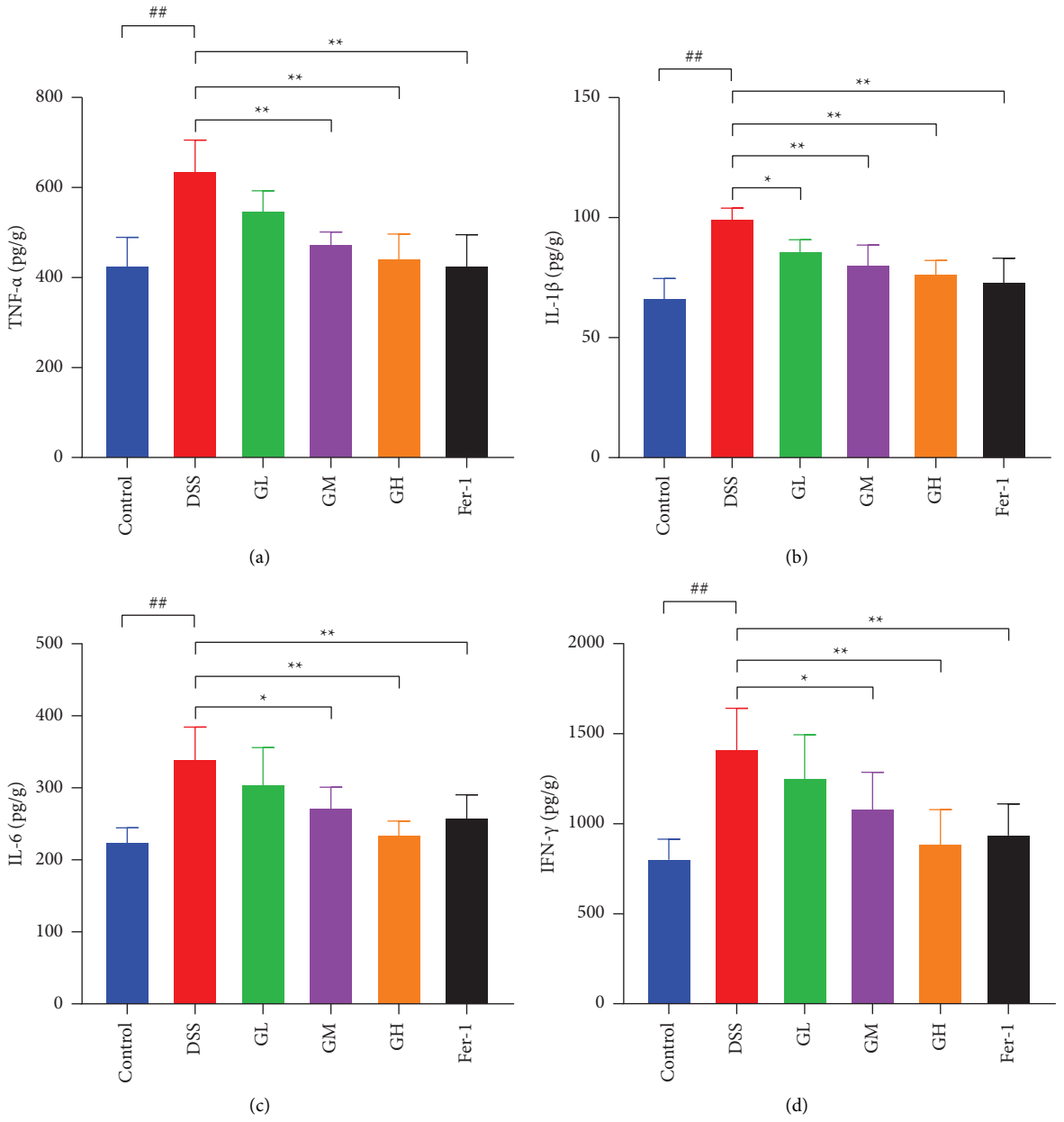

Figure 2: Levels of inflammatory cytokines in the colonic tissues of mice. Levels of (a) TNF-α, (b) IL-1β, (c) IL-6, and (d) IFN-γ ($n = 6$). $^{\#\#}P < 0.005$ vs. control; $^{*}P < 0.05$ vs. DSS; $^{**}P < 0.005$ vs. DSS.

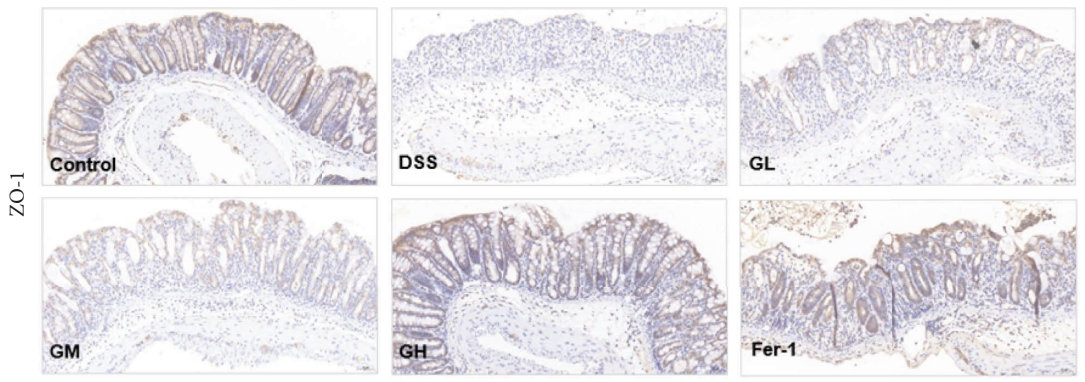

(a)

Figure 3: Continued.

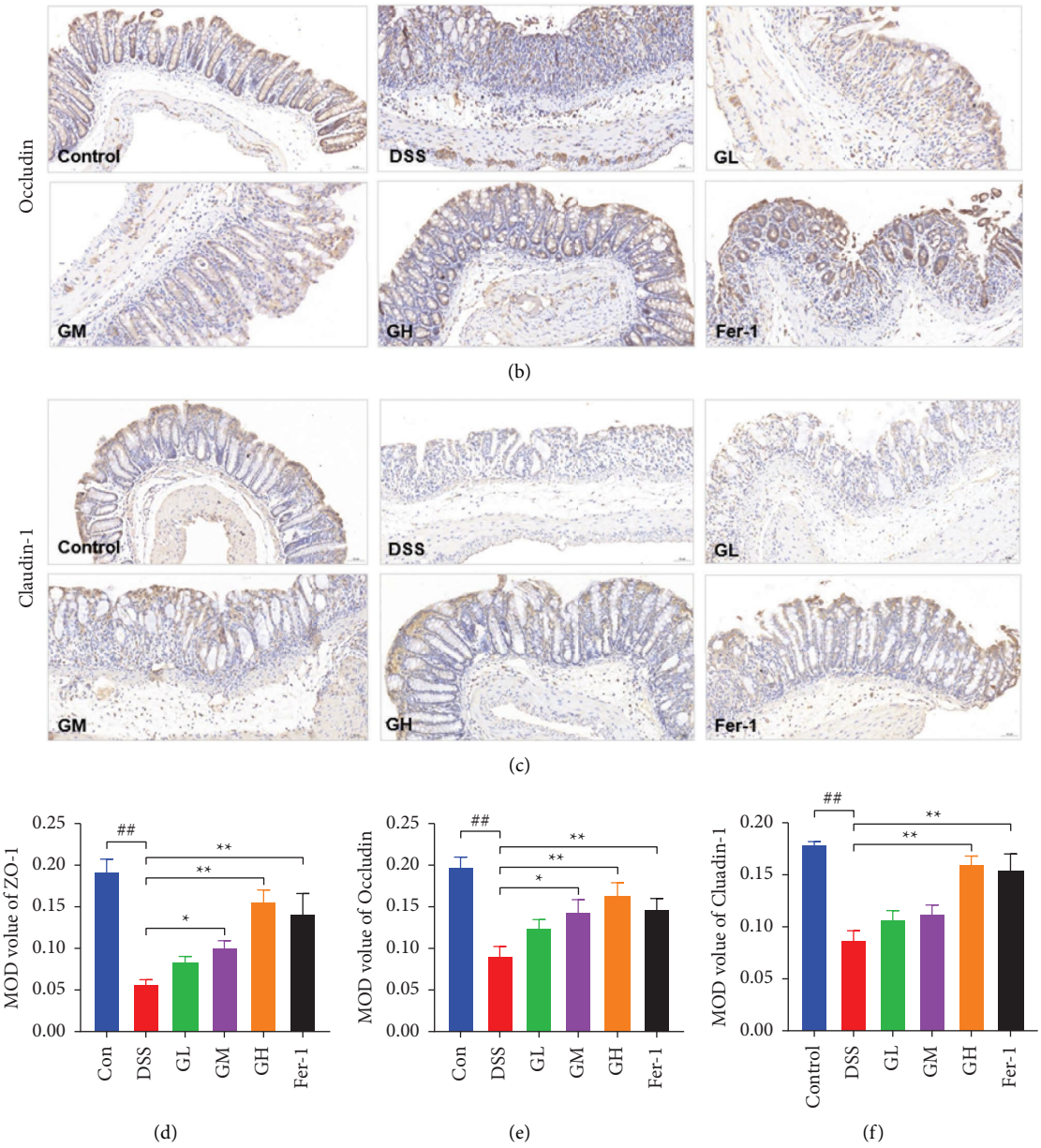

Figure 3: MGQD enhanced intestinal barrier in DSS-induced mice with UC. The expression of TJ proteins via immunohistochemical analysis (200x magnification): ZO-1 (a, d), occludin (b, e), and claudin-1 (c, f) in the colonic tissues of mice ($n = 6$). $^{\#\#}P < 0.005$ vs. control; $^{*}P < 0.05$ vs. DSS; $^{**}P < 0.005$ vs. DSS.

Interestingly, mice with UC who received MGQD exhibited a dose-dependent increase in Nrf2 and GPX4 expression levels (Figure 8). Furthermore, the levels of genes located downstream of Nrf2, namely, *SCL7A11* and *FTH1*, were notably increased after MGQD treatment.

3.6. Molecular Docking of MGQD and Nrf2. In molecular docking, the lower the energy needed for the ligand to bind to the receptor to form a conformation, the more stable the structure was. Our results (Table 2 and Figure 9) revealed that the binding energies of MGQD and Nrf2 were less than −5 kcal/mol, and at least one hydrogen bond was formed between them. This indicated that the main components of MGQD could stably bind to Nrf2, and MGQD may affect UC through the Nrf2 pathway.

4. Discussion

Traditional Chinese herbal medicines have been popular in these years for many diseases [17, 18]. As complementary and alternative therapies, traditional Chinese herbal medicines are considered promising adjuvant treatment options for colitis [19]. GQD is a well-known Chinese herbal formula beneficial for UC [12]. GQD has been reported to alleviate UC by modulating immune responses, inhibiting oxidative stress, promoting intestinal mucosal barrier repair, and regulating gut microbes [20–22]. As a modified herbal

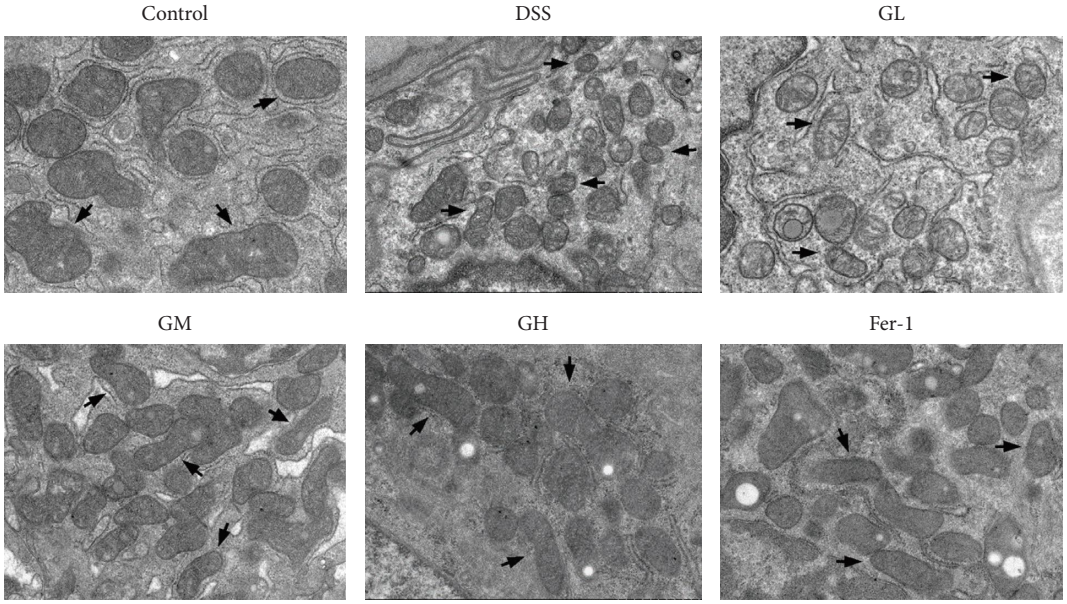

Figure 4: Representative transmission electron microscopic images of the mitochondria in colonic tissues of mice (black arrowheads, classical mitochondria in the soma; scale bars = 1 μm; $n = 3$).

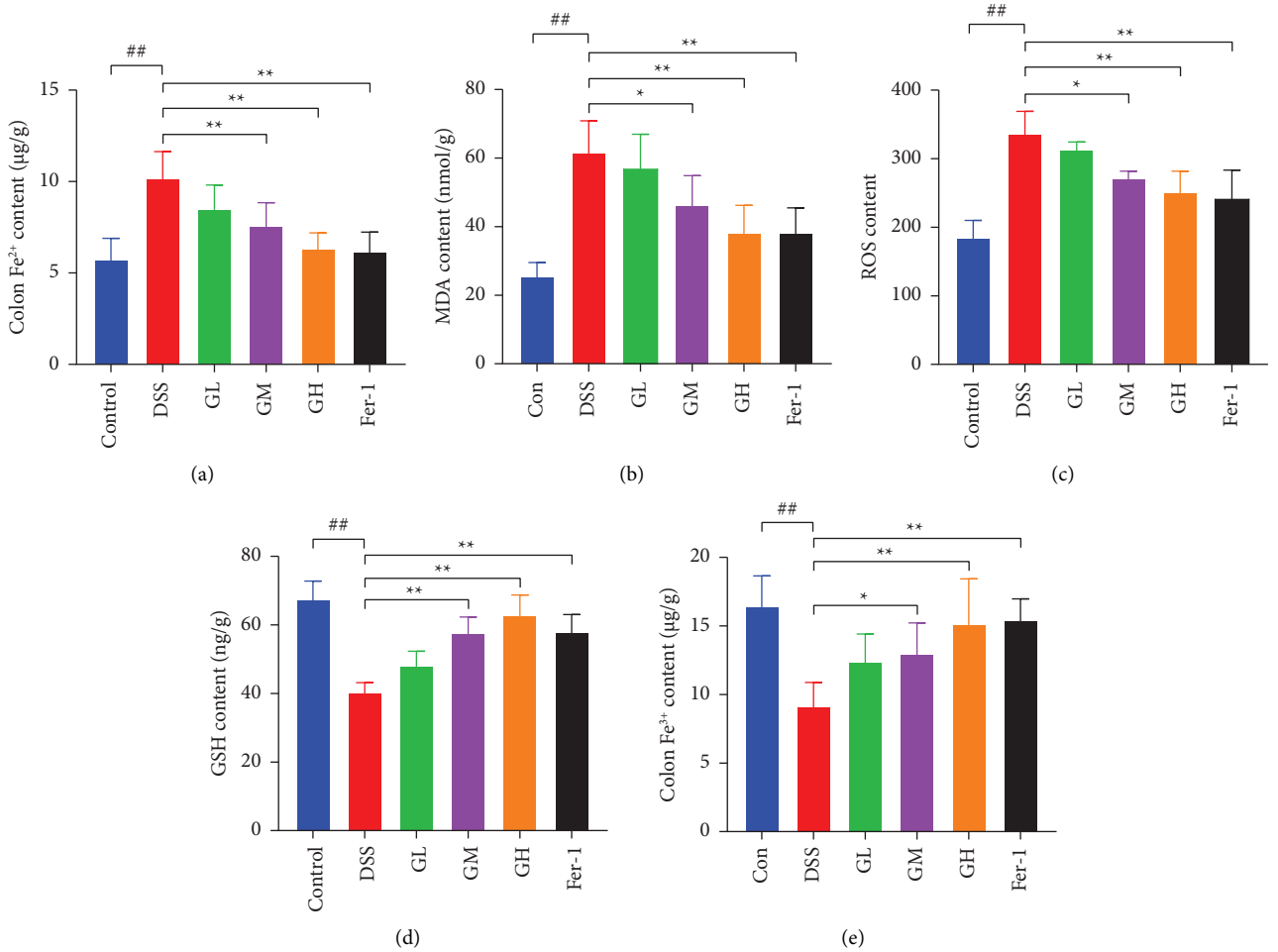

Figure 5: The lipid peroxidation and the level of iron load in colonic tissues. (a) Content of Fe^{2+}, (b) MDA levels, (c) ROS levels, (d) GSH levels, (e) content of Fe^{3+} ($n = 6$). $^{\#}P < 0.05$ vs. control, $^{\#\#}P < 0.005$ vs. control, $^{*}P < 0.05$ vs. DSS, $^{**}P < 0.005$ vs. DSS.

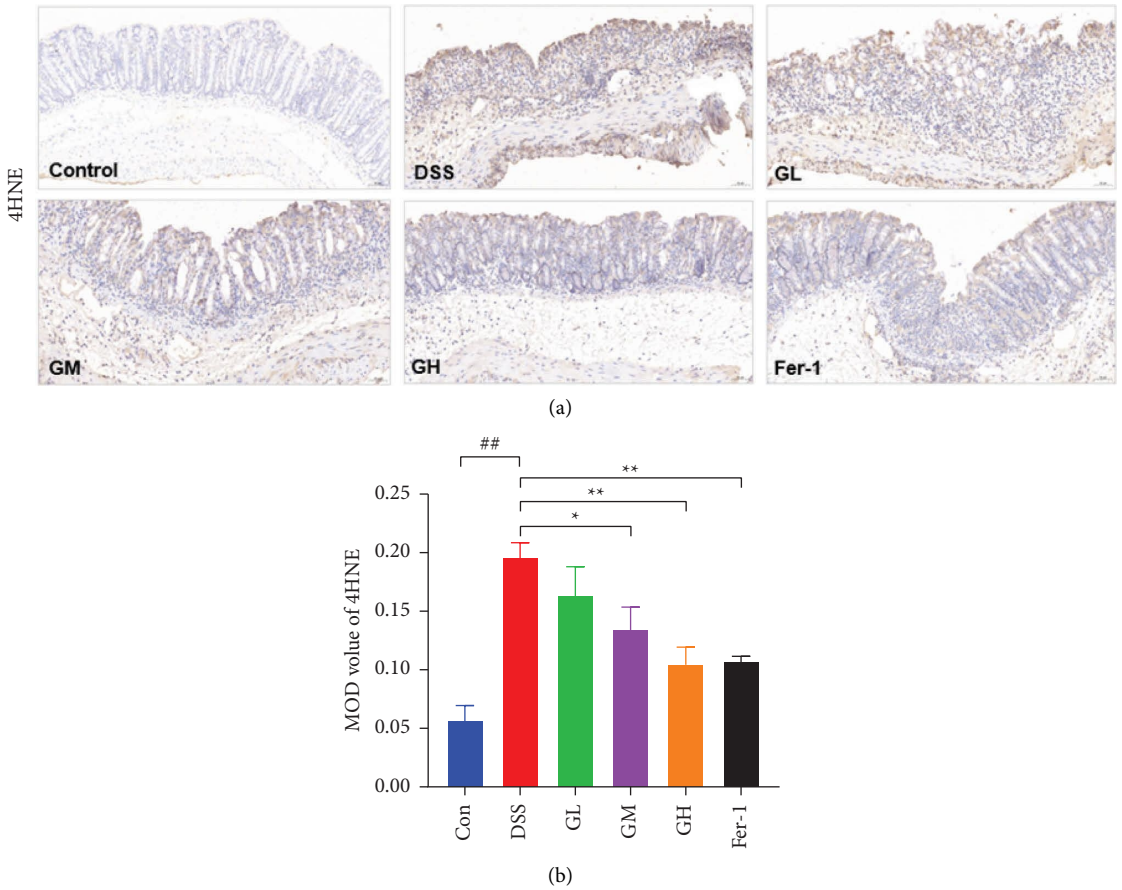

Figure 6: Representative images of immunohistochemical staining of 4HNE levels in colonic tissues ($n = 3$). $^{\#\#}P < 0.005$ vs. control; $^{*}P < 0.05$ vs. DSS; $^{**}P < 0.005$ vs. DSS.

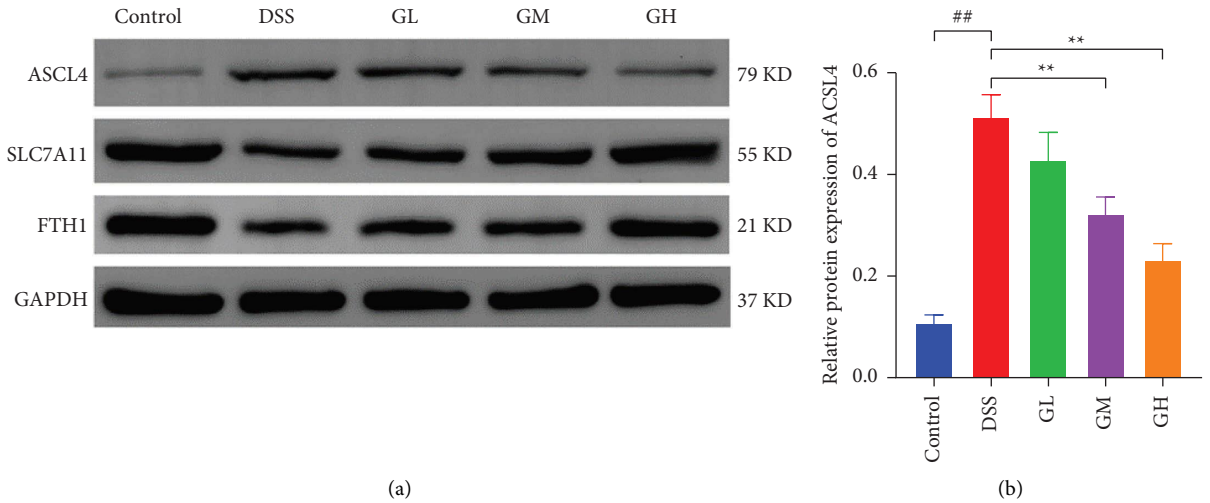

Figure 7: Continued.

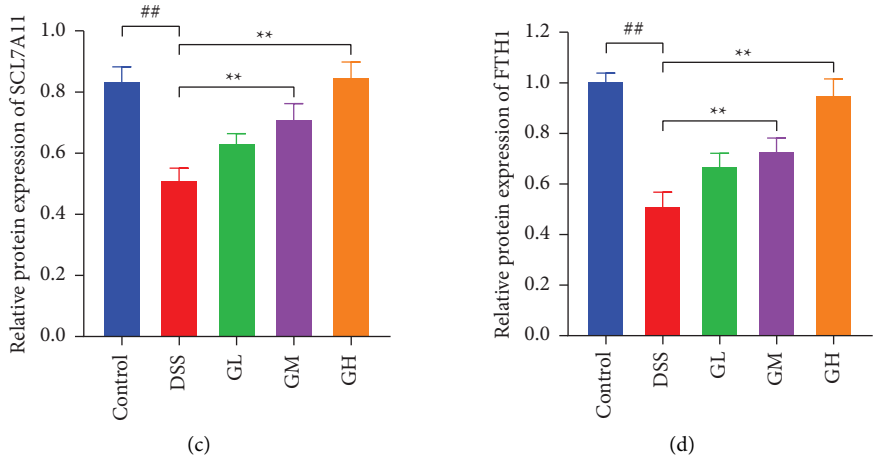

Figure 7: Protein expression of ACSL4, SLC7A11, and FTH1 determined using western blot analysis ($n = 3$). $^{\#\#}P < 0.005$ vs. control; $^{*}P < 0.05$ vs. DSS; $^{**}P < 0.005$ vs. DSS.

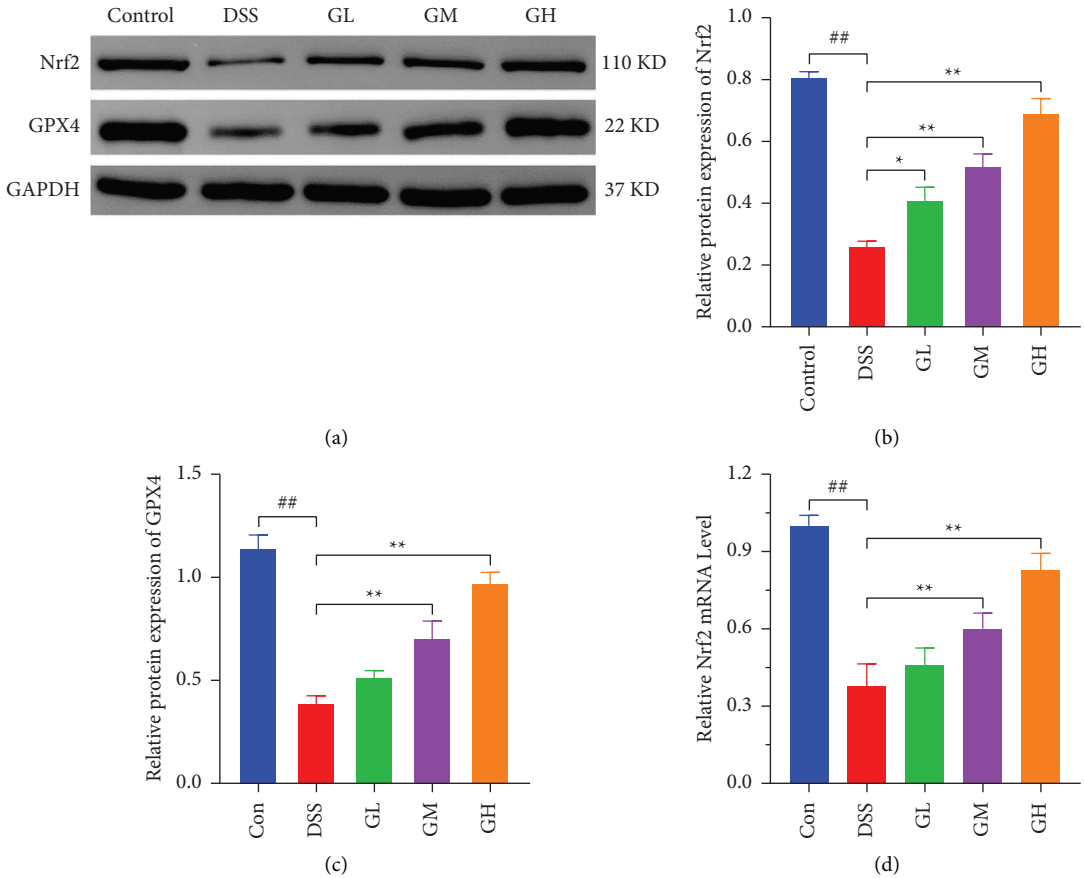

Figure 8: Continued.

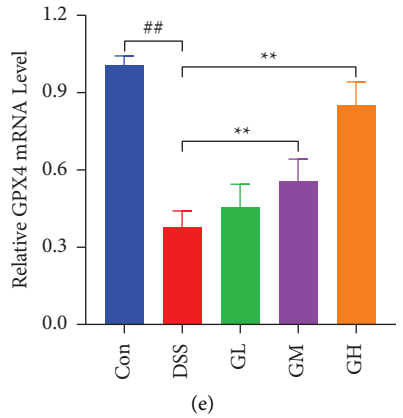

(e)

Figure 8: MGQD activated the Nrf2/GPX4 pathway in the colonic tissues of mice with UC. (a–c) Protein expression of Nrf2 and GPX4 determined using western blot analysis ($n = 3$). (d, e) mRNA level of GPX4 and FTH1 determined using RT-qPCR ($n = 6$). $^{\#\#}P < 0.005$ vs. control; $^{*}P < 0.05$ vs. DSS; $^{**}P < 0.005$ vs. DSS.

Table 2: Binding energy of components of MGQD and target protein.

Target	PDB IDs	Components	Docking energy (kcal/mol)
Nrf2	7k2n	Baicalin	−9.8
Nrf2	7k2n	Berberine	−9.7
Nrf2	7k2n	Palmatine chloride	−8.2
Nrf2	7k2n	Puerarin	−9.7
Nrf2	7k2n	Wogonin	−9.1

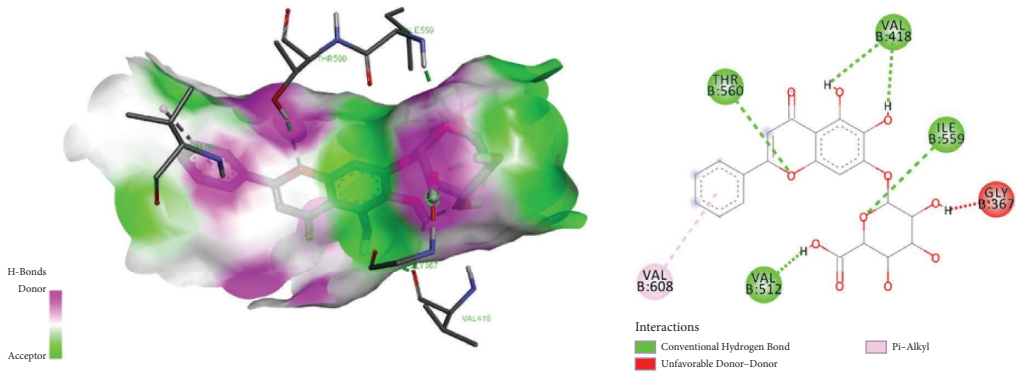

(a)

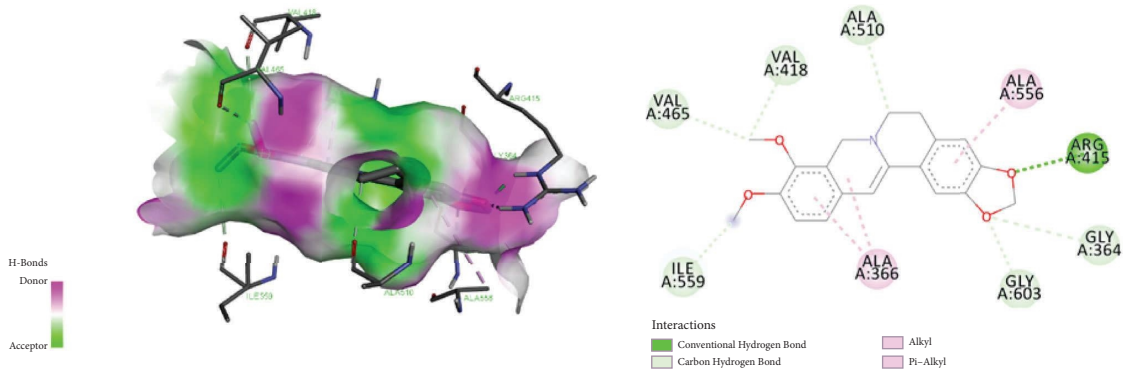

(b)

Figure 9: Continued.

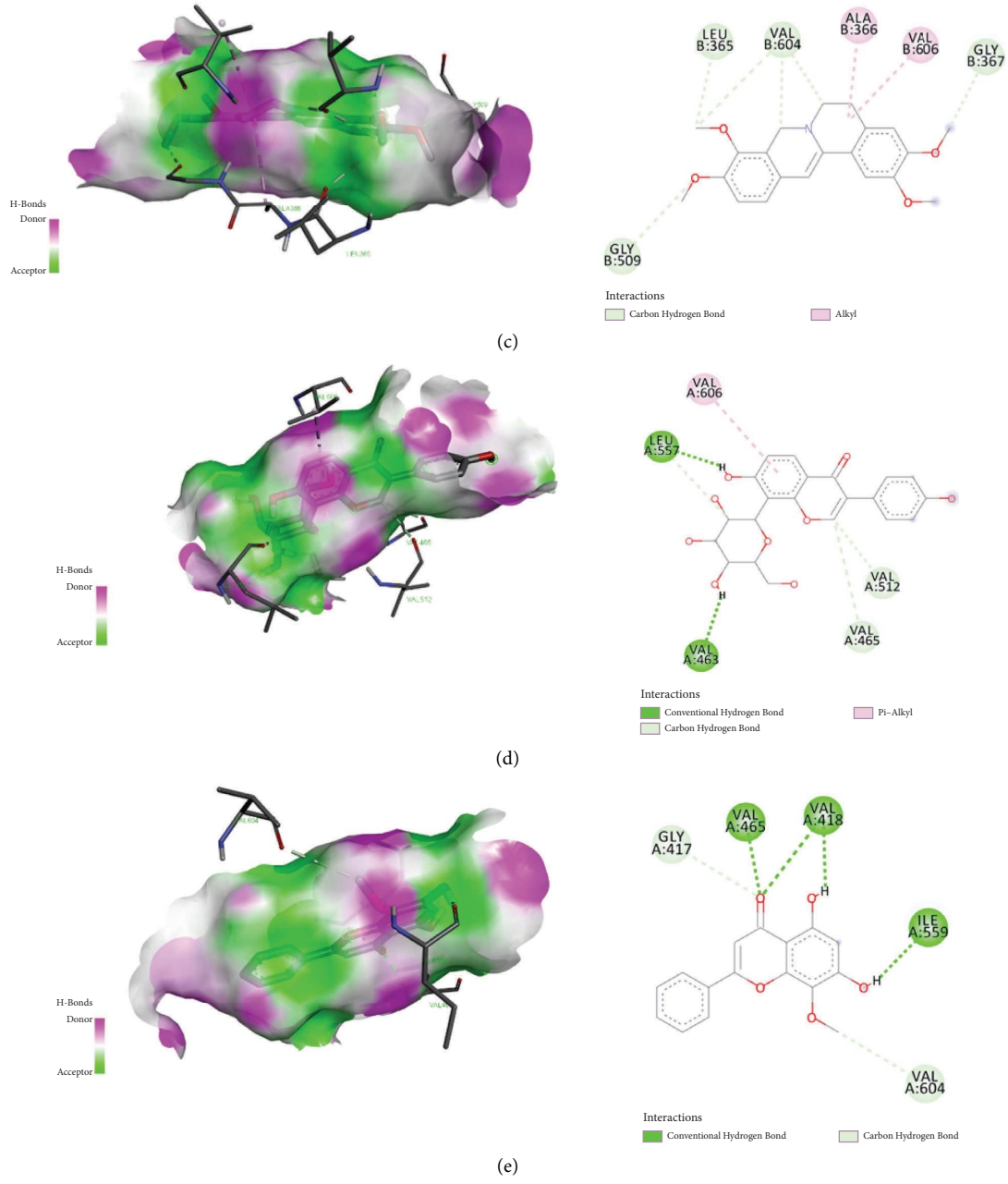

Figure 9: Docking models of components of MGQD to Nrf2. (a) binding of baicalin to Nrf2; (b) binding of berberine to Nrf2; (c) binding of palmatine chloride to Nrf2; (d) binding of puerarin to Nrf2; (e) binding of wogonin to Nrf2.

compound of GQD, MGQD has likewise been found to alleviate UC by modulating immunity, inhibiting oxidative stress, and regulating gut microbes [13–15]. Accumulating evidence suggested that epithelial cell injury is associated with ferroptosis in UC, and targeted inhibition of ferroptosis can help to promote repair of the intestinal mucosal barrier [22, 23]. Therefore, we aimed to explore whether MGQD can ameliorate UC via targeting the inhibition of ferroptosis through the establishment of an experimental mouse model with UC.

After 7 days of UC induction using DSS, mice in the DSS group developed characteristic symptoms of colitis, including blood in the stool, loose stools, weight loss, and shortening of the colon. In addition, pathological findings revealed an inflammatory infiltrate and mucosal damage in the colonic tissues of mice with UC, which corresponded to an increase in a large number of inflammatory cytokines and suppression of tight junction proteins. These results demonstrated that an experimental mouse model of UC had been successfully established. More importantly, the core characteristics of ferroptosis, such as lipid peroxidation accumulation, iron deposition, reduction in GPX4 activity and GSH level, and morphological changes in the mitochondria, were observed in the intestine of mice with UC. When the mice with UC were administered with Fer-1, a ferroptosis inhibitor, these core characteristics of ferroptosis were

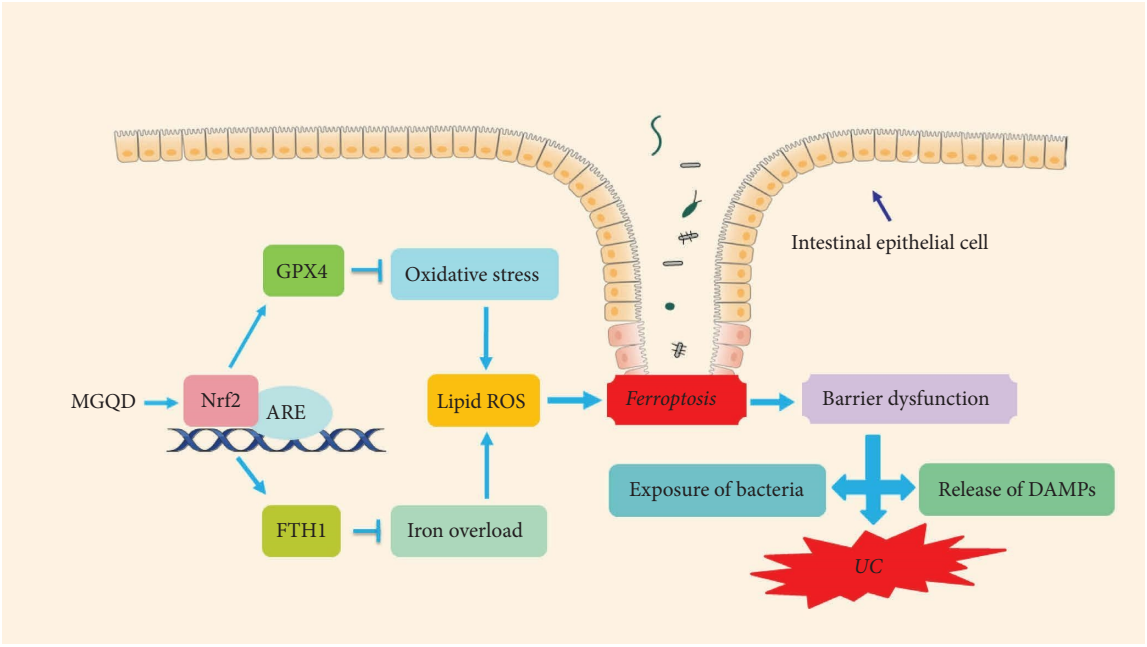

Figure 10: Mechanism of action of MGQD in ameliorating UC in mice via the inhibition of ferroptosis.

reversed and were accompanied by improvements in colitis symptoms, such as blood in stool, loose stools, weight loss, shortened colon, and inflammatory infiltration. The intestinal barrier breaks down as a result of intestinal epithelial cell death [24]. Interestingly, the levels of tight junction proteins were significantly restored after protecting the intestinal epithelium of mice with UC by inhibiting ferroptosis. These findings suggested that ferroptosis is associated with intestinal mucosal barrier breakdown in UC, and targeted inhibition of ferroptosis can help in alleviating colitis.

In this study, mice with UC treated with MGQD exhibited increased body weight, longer colon length, decreased DAI score, and improved pathology score, which is consistent with our previous findings [13–15]. More importantly, similar to Fer-1, the core characteristics of ferroptosis exhibited by mice with UC, such as lipid peroxide accumulation, iron deposition, reduced GSH levels, and mitochondrial morphological changes, were significantly reversed after treatment with MGQD. This suggested that MGQD inhibits ferroptosis in mice with UC. In addition, MGQD helped to promote the repair of the colonic mucosal barrier as the levels of tight junction proteins in the colonic tissues of mice with UC were restored after MGQD treatment.

Ferroptosis is characterized by iron overload and lipid accumulation [25]. The Nrf2 pathway is well known for its role in antioxidant defense [26, 27]. Notably, GPX4 is an established Nrf2 transcriptional target [28]. Therefore, activation of the Nrf2/GPX4 pathway is considered critical for the inhibition of ferroptosis [10, 11]. In this study, the Nrf2/GPX4 pathway was significantly inhibited in mice with UC, and the expression of the downstream genes of Nrf2, including *SCL7A11* and *FTH1*, was inhibited. When the Nrf2/GPX4 pathway is inhibited, indicators of lipid peroxidation including ACSL4 and 4HNE are significantly activated. Surprisingly, the Nrf2/GPX4 pathway and its downstream genes were activated in the colonic tissues of mice with UC after treatment with MGQD. In addition, the levels of ACSL4 and 4HNE, which are generally used as biomarkers of ferroptosis, were decreased in mice treated with MGQD. Additionally, the results of molecular docking revealed that Nrf2 could be stably bound to the components of MGQD. These findings suggested that MGQD inhibits ferroptosis via the Nrf2/GPX4 pathway to alleviate UC (Figure 10).

Limitations should be acknowledged. First, molecular docking was carried out based on the results of animal experiments, and the results obtained by the molecular docking method were not validated by in vitro experiments, and further exploration of the effects of the components of MGQD on the Nrf2 pathway on the basis of the UC model is still necessary in the future. Second, ferroptosis belongs to one of the forms of programmed cell death, and further studies to explore whether MGQD can regulate other forms of programmed cell death to alleviate UC are also necessary in the future.

5. Conclusion

In conclusion, our study demonstrated that ferroptosis is involved in DSS-induced UC in mice, and MGQD may exert anticolitis effect by inhibiting ferroptosis through the activation of the Nrf2/GPX4 pathway. These findings provided novel insights into the application of MGQD to ameliorate UC.

Abbreviations

UC: Ulcerative colitis
GQD: Gegen Qinlian decoction
MGQD: Modified Gegen Qinlian decoction

DSS: Dextran sulfate sodium
GM: Medium-dose MGQD
GL: Low-dose MGQD
GH: High-dose MGQD
Fer-1: Ferroprostatin-1
MDA: Malondialdehyde
GSH: Glutathione
ROS: Reactive oxygen species
H&E: Hematoxylin and eosin
DAI: Disease activity index
MOD: Mean optical density.

Data Availability

The datasets generated for this study are available upon request to the corresponding author.

Ethical Approval

This work was approved by the Animal Ethics Committee of Xiyuan Hospital of China Academy of Chinese Medical Sciences (Approval No. 2019XLC003-2).

Conflicts of Interest

The authors declare that there are no conflicts of interest.

Authors' Contributions

Jinke Huang designed the research, analyzed the data, and wrote the paper. Jinke Huang, Zhihong Liu, Jiaqi Zhang, Jing Ma, and Fengyun Wang performed the experiments. Xudong Tang contributed to review and editing.

Acknowledgments

We thank Bullet Edits Limited for the linguistic editing and proofreading of the manuscript. This work was supported by the National Natural Science Foundation of China (Nos. 82341233 and 81830118), China Academy of Chinese Medical Sciences Innovation Fund (No. CI2021A01012), China Academy of Chinese Medical Sciences Excellent Young Talent Cultivation Fund (No. ZZ15-YQ-002), and Administration of Traditional Chinese Medicine Digestive Refractory Disease Inheritance and Innovation Team Project (No. ZYYCXTD-C-202010).

References

[1] C. Le Berre, S. Honap, and L. Peyrin-Biroulet, "Ulcerative colitis," *The Lancet*, vol. 402, no. 10401, pp. 571–584, 2023.
[2] M. J. Buie, J. Quan, J. W. Windsor et al., "Global hospitalization trends for crohn's disease and ulcerative colitis in the 21st century: a systematic review with temporal analyses," *Clinical Gastroenterology and Hepatology*, vol. 21, no. 9, pp. 2211–2221, 2023.
[3] C. W. Ko, S. Singh, J. D. Feuerstein et al., "AGA clinical practice guidelines on the management of mild-to-moderate ulcerative colitis," *Gastroenterology*, vol. 156, no. 3, pp. 748–764, 2019.
[4] J. D. Feuerstein, K. L. Isaacs, Y. Schneider et al., "AGA clinical practice guidelines on the management of moderate to severe ulcerative colitis," *Gastroenterology*, vol. 158, no. 5, pp. 1450–1461, 2020.
[5] C. J. Ooi, I. Hilmi, R. Banerjee et al., "Best practices on immunomodulators and biologic agents for ulcerative colitis and Crohn's disease in Asia," *International Researchers*, vol. 17, no. 3, pp. 285–310, 2019.
[6] U. N. Shivaji, C. L. Sharratt, T. Thomas et al., "Review article: managing the adverse events caused by anti-TNF therapy in inflammatory bowel disease," *Alimentary Pharmacology and Therapeutics*, vol. 49, no. 6, pp. 664–680, 2019.
[7] D. Tang, X. Chen, R. Kang, and G. Kroemer, "Ferroptosis: molecular mechanisms and health implications," *Cell Research*, vol. 31, no. 2, pp. 107–125, 2021.
[8] M. Xu, J. Tao, Y. Yang et al., "Ferroptosis involves in intestinal epithelial cell death in ulcerative colitis," *Cell Death and Disease*, vol. 11, no. 2, p. 86, 2020.
[9] J. Huang, J. Zhang, J. Ma et al., "Inhibiting ferroptosis: a novel approach for ulcerative colitis therapeutics," *Oxidative Medicine and Cellular Longevity*, vol. 2022, Article ID 9678625, 9 pages, 2022.
[10] J. Wang, Q. Zhu, Y. Wang, J. Peng, L. Shao, and X. Li, "Irisin protects against sepsis-associated encephalopathy by suppressing ferroptosis via activation of the Nrf2/GPX4 signal axis," *Free Radical Biology and Medicine*, vol. 187, pp. 171–184, 2022.
[11] C. Wang, S. Chen, H. Guo et al., "Forsythoside A mitigates alzheimer's-like pathology by inhibiting ferroptosis-mediated neuroinflammation via nrf2/GPX4 Axis activation," *International Journal of Biological Sciences*, vol. 18, no. 5, pp. 2075–2090, 2022.
[12] J. Huang, J. Zhang, Y. Wang et al., "Scientific evidence of Chinese herbal medicine (gegen qinlian decoction) in the treatment of ulcerative colitis," *Gastroenterology Research and Practice*, vol. 2022, pp. 1–8, 2022.
[13] Y. Wang, J. Zhang, L. Xu et al., "Modified gegen qinlian decoction regulates treg/Th17 balance to ameliorate DSS-induced acute experimental colitis in mice by altering the gut microbiota," *Frontiers in Pharmacology*, vol. 12, Article ID 756978, 2021.
[14] Y. Wang, J. Zhang, B. Zhang et al., "Modified Gegen Qinlian decoction ameliorated ulcerative colitis by attenuating inflammation and oxidative stress and enhancing intestinal barrier function in vivo and in vitro," *Journal of Ethnopharmacology*, vol. 313, Article ID 116538, 2023.
[15] J. Ma, J. Zhang, Y. Wang et al., "Modified Gegen Qinlian decoction ameliorates DSS-induced chronic colitis in mice by restoring the intestinal mucus barrier and inhibiting the activation of $\gamma\delta$T17 cells," *Phytomedicine*, vol. 111, Article ID 154660, 2023.
[16] A. Yokote, N. Imazu, J. Umeno et al., "Ferroptosis in the colon epithelial cells as a therapeutic target for ulcerative colitis," *Journal of Gastroenterology*, vol. 58, no. 9, pp. 868–882, 2023.
[17] Q. Zheng, Y. Gao, X. Lu et al., "Chinese herbal medicine and COVID-19: quality evaluation of clinical guidelines and expert consensus and analysis of key recommendations," *Acupuncture and Herbal Medicine*, vol. 2, no. 3, pp. 152–161, 2022.
[18] Y. Qi, M. Wang, L. Chai et al., "Wei Chang an pill alleviates 2,4,6-trinitro-benzenesulfonicacid-induced ulcerative colitis by inhibiting epithelial-mesenchymal transition process," *Acupuncture and Herbal Medicine*, vol. 3, no. 2, pp. 107–115, 2023.

[19] Y. Liu, B. G. Li, Y. H. Su et al., "Potential activity of traditional Chinese medicine against ulcerative colitis: a review," *Journal of Ethnopharmacology*, vol. 289, Article ID 115084, 2022.

[20] R. Li, Y. Chen, M. Shi et al., "Gegen Qinlian decoction alleviates experimental colitis via suppressing TLR4/NF-κB signaling and enhancing antioxidant effect," *Phytomedicine*, vol. 23, no. 10, pp. 1012–1020, 2016.

[21] Y. Zhao, H. Luan, H. Jiang et al., "Gegen Qinlian decoction relieved DSS-induced ulcerative colitis in mice by modulating Th17/Treg cell homeostasis via suppressing IL-6/JAK2/STAT3 signaling," *Phytomedicine*, vol. 84, Article ID 153519, 2021.

[22] X. Wang, S. Huang, M. Zhang et al., "Gegen Qinlian decoction activates AhR/IL-22 to repair intestinal barrier by modulating gut microbiota-related tryptophan metabolism in ulcerative colitis mice," *Journal of Ethnopharmacology*, vol. 302, no. Pt B, Article ID 115919, 2023.

[23] H. Chen, Y. Qian, C. Jiang et al., "Butyrate ameliorated ferroptosis in ulcerative colitis through modulating Nrf2/GPX4 signal pathway and improving intestinal barrier," *Biochimica et Biophysica Acta- Molecular Basis of Disease*, vol. 1870, no. 2, Article ID 166984, 2024.

[24] W. Gao, T. Zhang, and H. Wu, "Emerging pathological engagement of ferroptosis in gut diseases," *Oxidative Medicine and Cellular Longevity*, vol. 2021, Article ID 4246255, 16 pages, 2021.

[25] J. Wan, H. Ren, and J. Wang, "Iron toxicity, lipid peroxidation and ferroptosis after intracerebral haemorrhage," *Stroke Vasc Neurol*, vol. 4, no. 2, pp. 93–95, 2019.

[26] F. Manai and M. Amadio, "Dimethyl fumarate triggers the antioxidant defense system in human retinal endothelial cells through Nrf2 activation," *Antioxidants*, vol. 11, no. 10, 2022.

[27] T. Wang, Z. Jian, A. Baskys et al., "MSC-derived exosomes protect against oxidative stress-induced skin injury via adaptive regulation of the NRF2 defense system," *Biomaterials*, vol. 257, Article ID 120264, 2020.

[28] Y. Wang, S. Yan, X. Liu et al., "PRMT4 promotes ferroptosis to aggravate doxorubicin-induced cardiomyopathy via inhibition of the Nrf2/GPX4 pathway," *Cell Death and Differentiation*, vol. 29, no. 10, pp. 1982–1995, 2022.